Evaluation of Power Generation Potential of Cellulose Microfibrils and Onion Skin-based Bio-Piezoelectric Nanogenerators

Juan Camilo Botín Sanabria[a]

Davinson Castaño Cano[b]

[a] *Process Engineering Student, EAFIT University, Medellín, Colombia*
[b] *Professor, Bachelor's degree projet advisor, Department of Production Engineering, EAFIT University, Medellín, Colombia*

Abstract

It is highly desirable for new nanosystems and nanodevices to be self-powered for applications in biomedical science, sensing, robotics and personal electronics. As new trends require these devices to be downsized and incorporated in remote and hard to reach locations the challenge to develop new technologies that allow autonomous, maintenance-free and continuous supply of energy is great. Over the last decade researchers have found ways to harness ambient energy from mechanical vibrations to develop self-powered devices. The present research reports the fabrication of two bio-piezoelectric generators using cellulose as biomaterial in two distinct configurations, as well as commonly used materials in a simple manufacturing process. Cellulose microfibrils, a disoriented structure, obtained from cotton wads was mixed with silicone to obtain an CMFPNG, while onion skin, a more oriented cellulose structure, was left untreated or naked to fabricate a NOSBPNG. The chemical and physical differences where evaluated using Fourier-transform Infrared Spectroscopy (FTIR) and Scanning Electron Microscopy (SEM), the abundance of H-boding groups available in the onion skin structure present an interesting proposition for a high performance piezoelectric material, while the simpler an disoriented fashion on CMFs is less likely to perform equally. The self-orientation of PNG using onion skin without chemical treatment and no sputtering for the formation of the electrode generate an output voltage up until 3.26 V and store 0.395 V in a 4.7 μF capacitor, resulting in a power storage of 1.25 μJ, making it a viable material for the construction of smart devices such as PNG. CMFPNG results were not conclusive, hence it is suggested the present methods are not the adequate for this material. However important factors to consider are presented for future research. Nevertheless the results of NOSBPNG support the use of onion skin as a self-oriented waste material for the construction of new smart bio-materials.

1. Introduction

Progress in the development of new autonomous, sustainable, maintenance free and continuous, robots, implantable medical devices (IMDs), micro-sensors, wireless sensor networks (WSN), micro-electromechanical systems (MEMS) and next generation portable devices, has intensified the necessity of supplying energy at smaller scales. New trends require the downsize of these devices and their use in remote or hard to reach locations, these restrictions increase the difficulty to supply electrical power [1]–[3]. Conventional systems are powered by complex wiring systems or onboard batteries, made from contaminant materials, they are also bulky and need constant replacement [4], [5]. To overcome these issues energy harvesting (EH) devices are a fitting solution. Researchers have found ways to "harvest" or "scavenge" energy from ambient sources such as: light, heat, mechanical vibrations, radio frequency (RF) and magnetic effects, amongst others [1], [6].

Since energy is a vital element across numerous fields, EH has become an important focus of research over the last decade [7]. Photovoltaic energy harvesting is the most efficient method to produce electrical power

when it is harnessed outdoors, however its performance decreases greatly in closed environments, which means it is not suitable for continuous operation [8]. Other technologies such as RF are still in early stages of development and presents low power densities [9]. Thermoelectric devices present some drawbacks in some applications, such as the solid state and bulky structure [10]. Harvesting energy from mechanical vibrations results viable since in indoor locations and it can be found in nearly all the environments were these applications could be implemented. Ambient vibrations are present in machinery, roads, windows, water and even the human body (e.g. arterial pulse, throat sounds, heartbeat and overall motion) [11]–[13].

Mechanical energy harvesters employ on of the following transducer technologies: electrostatic, electromagnetic and piezoelectric. Electrostatic harvesters need a separate voltage sources which increase the size of the device, making them incompatible with certain applications, besides they have small power densities. Electromagnetic harvesters can lead to complex architectures for small applications, incrementing assembly and maintenance costs [2], [14]. On the other hand, piezoelectric harvesters are structurally simpler, because they rely on smart piezoelectric material which can be manufactured in thin films that greatly reduce the size and can produce higher power densities than their counterparts [15]. Piezoelectric materials produce electrical charge when they are subject to mechanical stress or strain, this is known as the direct piezoelectric effect, inversely these materials can be strained when an electric field is applied, this in known as the inverse piezoelectric effect [16].

Most commercial piezoelectric materials are inorganic and although they have higher electromechanical responses, they are also toxic, mechanically hard and brittle, making them incompatible for certain applications. Some common piezoelectric materials are: barium titanate ($BaTiO_3$), zinc oxide (ZnO) and lead zirconate titanate (PZT) [17]. In the current context other characteristics are needed for these materials such as being thin, flexible, mechanically stretchable, soft, led-free and biocompatible [18]. New materials and techniques have been studied to build piezoelectric generators with interesting results, however, at the time of these research no direct comparison of the physicochemical and electric characteristics has been made between for these materials and their properties. Although important steps have been made to find feasible alternatives to replace the current ceramic piezoelectric materials, the technologies are still not available for massive production or commercialization, which highlights the importance to continue researching in this field.

For many decades the use of natural materials in electronics has been studied. Non-synthetic biocompatible piezoelectric materials have attracted the interest of researchers to replace inorganic and other synthetic materials. Proteins such as silk [19], [20] and polymers like cellulose and collagen and chitin, are the ones that have been studied the most [21]–[24]. These materials offer big advantages over those commonly used since they are biocompatible and biodegradable.

Collagen is one of the most abundant natural occurring piezoelectric materials in the world, as it is the most abundant structural protein of the animal connective tissue [17], [23]. Ghosh and Mandal [17] built a self-powered bio-e-skin with fish gelatin, using electrospinning technology. Goés et al. [25] studied the physiochemical, dielectric and piezoelectric properties of anionic and native collagen films, suggesting that the material can be used in sensing and energy harvesting applications. Chitin, found naturally in the exoskeletons of crustaceans, insects and fungi and commercially it is found as chitosan, presents attractive physical and chemical properties, such as biocompatibility biodegradability, non-toxicity and ease of film formation. Praveen et al. [26] investigated the existence of non-centrosymmetry of chitosan as well as its piezoelectric properties. Kim et al. [27] demonstrated the piezoelectricity in crystalline β-rich chitin materials, their findings remark the possibilities of using this material in eco—friendly piezoelectric generators and transductors.

Cellulose is the most abundant natural biopolymer and it exhibits both direct and indirect piezoelectric effects. This material is attractive due to a high piezoelectric coefficient, flexibility and other mechanical properties, additionally it can be easily collected as raw material since it can be found as a waste product in many industries [28] . Although the piezoelectricity of wood has been known for decades ways to enhance its piezoelectric effect have been studied, breaking down cellulose into more compact blocks such as cellulose microfibrils (CMFs), nanofibrils (CNFs) and cellulose nanocrystals (CNCs) and the inclusion of conducting fillers [29], [30]. Qifeng et al. [26] developed a high-performance flexible piezoelectric nanogenerator using

CNF/poly(dimethilsyloxane) (PDMS) aerogel film. Rajala et al. [28] synthesized native CNF films and studied its microstructure, piezoelectric and dielectric properties. These characterizations suggest that nanocellulose is an exciting new piezoelectric material. In a simple method, avoiding other chemical substances Alam and Mandal [29] prepared a flexible film by dispersion of native cellulose microfiber, as piezoelectric material, in a host polymer.

The current project consists on evaluating the potential of electric generation of non-synthetic biocompatible piezoelectric materials analyzing physicochemical and electrical characteristics. Two piezoelectric nano generators were constructed; naked onion skin bio piezoelectric generator (NOSBPNG) and cellulose microfibril piezoelectric generator, and their electrical characteristics were compared.

2. Materials and methods (1522)

2.1. Cellulose microfibrils (CMF) extraction from cotton

CMF were prepared from cotton. The methodology suggested by Rahbar et al. [1] was conducted with slight modifications. First, 5.0 g of 100% natural cotton wads, from Tecnoquímicas ®, were cut by hand into smaller less tangled pieces. The cotton was then mixed with 100 mL of 6.5M sulfuric acid, from Protokímica ®, stirred vigorously at 50°C using a Cornig PC-420D heating plate, for 4 hours. After the reaction time had passed the solution was added to 500 mL of cold distilled water to stop the reaction. The mixture was then blended during 2 minutes in the highest speed setting of an Osterizer ® Classic Blender. Afterwards the CMF where filtered using a Boeco R-300 vacuum pump and distilled water was added periodically until pH was neutral. The resulting CMF were then dried for 24 hours in a Heraeus Instruments Function Line convection oven at 40°C and stored at that temperature until they were used. Figure 1 shows images of the described process.

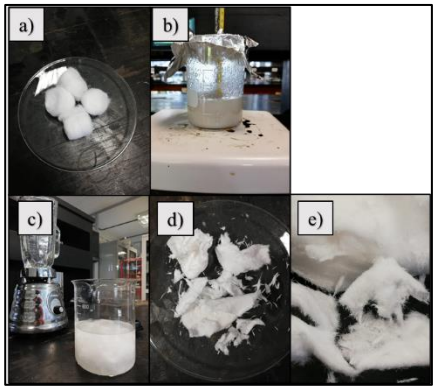

Figure 1 Schematic of CMF preparation. a) Cotton wads. b) Cotton and sulfuric acid reaction. c) Blended mixture. d) CMFs before drying. e) Dried CMFs close-up.

2.2. Onion skin preparation

The onion skin (OS) was obtained from red onions (Allium cepa) purchased in local supermarkets in the city of Medellín, which were sourced from different regions of Colombia. OS was cut into pieces of approximately 30 mm x 15 mm using regular scissors and a scalpel. The average thickness of the OS was ≈ 240 nm. The material was the dried at room temperature for 12 hours while being pressed with weights to ensure even flat surfaces. Figure 2 shows the dried onion skin.

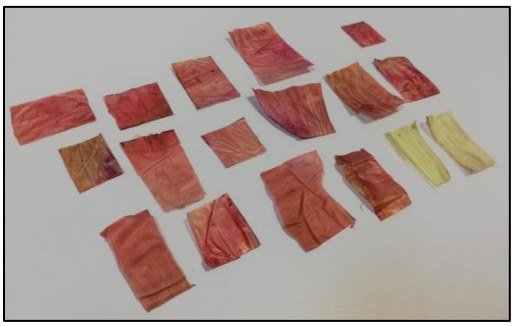

Figure 2 Dried onion skin

2.3. Physicochemical characterization

The CMFs samples obtained from the extraction process and the OSs were observed under scanning electron microscopy (SEM) with a SEM microscope FEI model Phenom, to determine the physical structure. Both materials were observed using Fourier-transform infrared spectroscopy (FTIR) with a FTIR spectrometer Nicolet iS20 to determine the characterize and identify the different functional groups in the samples. Both tests were performed in the facilities of EAFIT University following the required standards. The size determination of the fibrils structure was performed using freeware software ImageJ.

2.4. Onion skin bio-piezoelectric nanogenerator (NOSBPNG) fabrication

The fabrication process for the OSBPNG was a modified version of the one performed by Maiti et al. [2]. Two different nanogenerator were made with the following procedures, to identify them two terms were introduced: naked onion skin (NOS) and sputtered onion skin (SOS).

To build SOS bio-piezoelectric nanogenerators both sides of pieces of OS were sputtered with by Gold-Palladium (Au-Pd) coating to form the electrode. The onion pieces were placed in a Quorum SC7620 sputter coater system. The maximum time the OS samples could remain without degrading in the sputtering systems is 90 seconds, however due to the characteristics of the system 90 seconds yield between 12 and 30 nm in coating thickness. To overcome this inconvenience four depositions of 90 seconds each, separated by one minute between them, were carried to achieve an overall thickness between 48 and 120 nm, as seen in Figure 3.

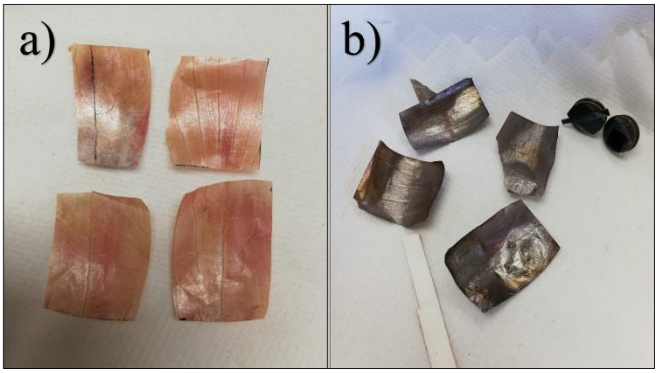

Figure 3 SOS generation. a) Dried onion skin (OS) b) Au-Pd sputtered onion skin (SOS).

According to the literature it was suggested to attach copper wires to the bottom and top electrodes using silver paste. However due to the elevated cost of the silver paste it was necessary to find other less expensive solutions, thus using copper (Cu) tape was suggested. Two different configurations were designed and built: a rigid and a flexible one. The rigid configuration consisted in Cu tape strips pasted to an acrylic surface 30 mm x 20 mm x 20 mm and then joined using insulating tape, as shown in Figure 4, respectively.

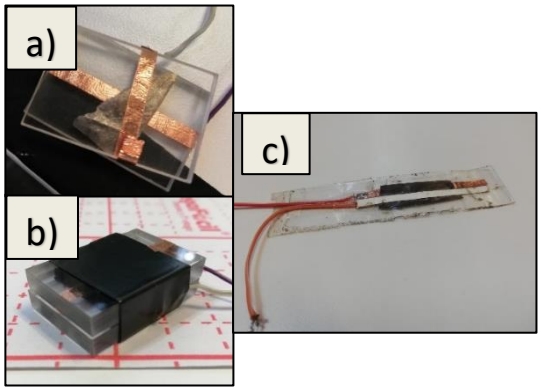

Figure 4 OSBPNG construction. a) Acrylic, Cu tape and SOS. b) Rigid OSBPNG - SOS rigid configuration. c) OSPNG - SOS flexible configuration.

Literature recommends protection of the material using PDMS, due to its elasticity, transparency and the conformal contact made between the surfaces [34]. However, OS with electrodes were protected using flexible and transparent contact paper. The direct contact between Cu tape electrodes and contact paper can generate a possible triboelectric charge. To avoid this shortcoming polypropylene tape was used as an intermediate layer between the Cu tape electrodes and the contact paper. The flexible configuration consisted in sandwich like formation using contact paper, Cu tape and SOS as shown in Figure 4. Frontal lateral and frontal views of the flexible device are shown in Figure 5, respectively. For both configurations the Cu wires were welded to the Cu tape using zinc.

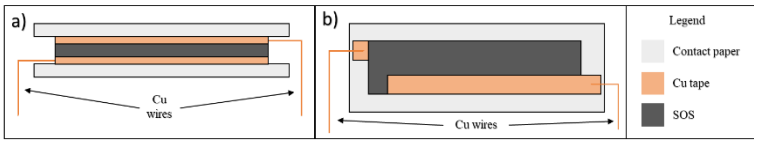

Figure 5 Flexible OSBPNG with SOS. a) Lateral view. b) Superior view.

As its name suggest NOS bio-piezoelectric nanogenerators, operate using OS without Au-Pd sputtered electrodes. Instead the OS is left without chemical or physical modifications and Cu tape is pasted to its surface to form the electrodes, as it is shown in Figure 6 . In the same way as the OSBPNG – SOS devices were built, Cu wires were soldered to the Cu tape electrodes, the resulting device is shown in Figure 6. Before device encapsulation in contact paper, polypropylene (PP) tape was used to cover the electrodes to avoid charges being generated on the contact paper surface. Frontal lateral and frontal views of the flexible device are shown in, Figure 7 respectively.

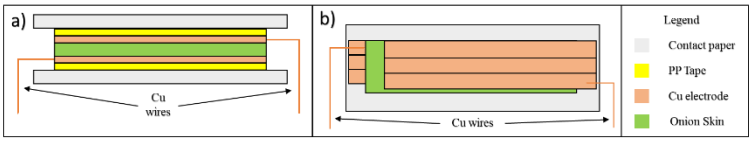

Figure 7 Flexible NOSBPNG.a) Lateral view. b) Superior view.

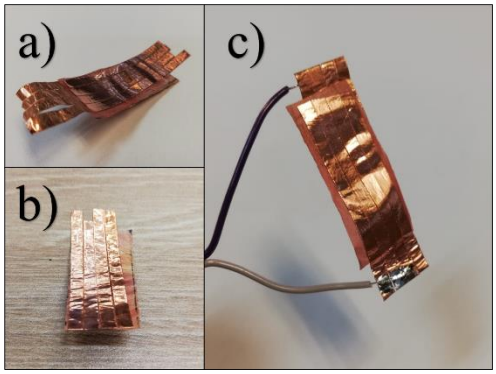

Figure 6 NOSBPNG device construction. a) Flexible NOS, b) Flexible NOS, c) Wired Flexible NOS

2.5. Cellulose microfibril piezoelectric nanogenerator (CMFPNG) fabrication

The schematic of the construction of the CFMPNG is shown in Figure 8. The fabrication process for the CMFPNG was a modified version of the one published by [30]. The authors suggested dispersion of CMFs in PDMS due to its elasticity, transparency and biocompatibility, as well as its capability to undergo *bulk modifications*. This modifications can alter and improve properties like thermal conductivity, elasticity and most importantly electric conductivity [34]. Literature suggests the incorporation of multiwall carbon nanotubes (MWCNT) as a conducting filler, which would also help the dispersion of CMFs in the PDMS matrix. However, for this investigation biocompatibility, a mayor motive for PDMS use, was not a requirement in addition to the high cost of this material compelled the search for a solution. Silicones are polymers that have a —R_2Si—O unit and PDMS is the simplest form of silicone with a —$Si(CH_3)_2$—O unit [30], [34]. Hence commercially available silicone was used to replace PDMS as the polymer matrix holding the cellulose microfibers. MWCNT were not used in this investigation.

First CMFs were dispersed in silicone by mechanical agitation in a 5:100 weight ratio as seen in Figure 8. Then the solution was poured in a cast shown in Figure 8 and Figure 9. As shown in there figures the base of the cast is made of a layer of Cu tape, forming the bottom electrode, likewise once the solution is poured the top electrode was put in place. Over both electrodes, PP tape was placed to avoid triboelectric charges generating on the surface of the electrodes and contact paper. Once the solution is poured into the cast, the bubbles were removed using a Boeco R-300 vacuum pump and then dried at room temperature for 12 hours. Cu cables were soldered to the Cu tape electrodes and protected using contact paper. The procedure to protect the piezoelectric film, was the same as in OSBPNG fabrication, hence before contact paper encapsulation PP

tape was used on top of the electrodes. Frontal lateral and frontal views of the flexible device are shown in, Figure 10 respectively. Figure 11 shows the result of CMFPNG fabrication.

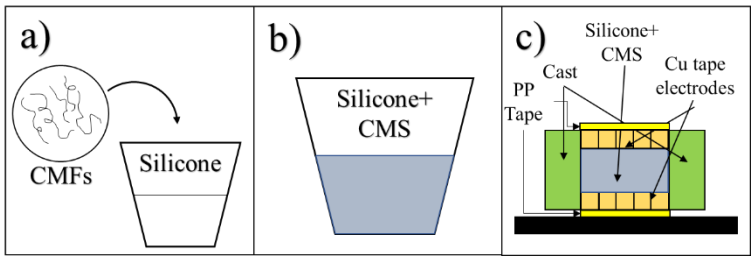

Figure 8 Schematic of CFMPNG fabrication. a) CMFs dispersion in silicone matrix. b) Silicone and CMFs mixture. c) Silicone and CMFs mixture are poured in a cast with Cu tape electrodes.

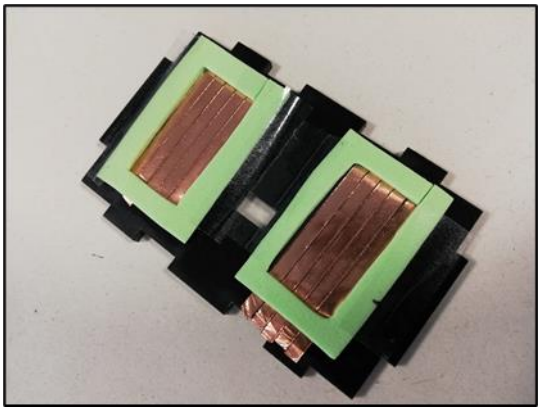

Figure 9 Casts for CMFPNG fabrication

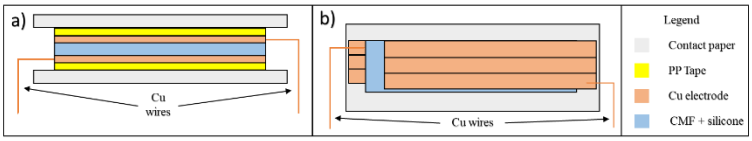

Figure 10 Flexible CMFPNG with SOS. a) Lateral view. b) Superior view.

Figure 11 CMFBPNG

2.6. Electrical measurements

To evaluate the power generation potential of both piezoelectric nanogenerators the circuits shown in Figure 12 were constructed. A four-diode bridge was used to rectify the AC current to DC current. Figure 12 indicates the use of a capacitor, which was used to measure the charging voltage; 4.7, 10 and 22 µF capacitors were used. The electrical outputs were measured by a digital oscilloscope Tektronix TBS 1052B-EDU and a digital multimeter UNI-T UT33C. Literature suggest the use of a current amplifiers, this will allow for proportional voltage measurements for a given current, since PNG generate small currents, this devices are used to obtain better readings, however in the present investigation, no current amplifiers were used.

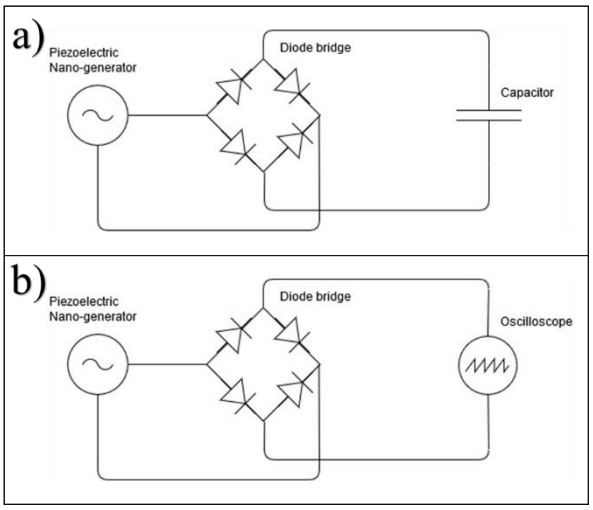

Figure 12 Circuit diagrams. a) charging voltage measurement. b) rectified voltage measurement.

2.7. Calculations for applied pressure

The pressure applied to the piezoelectric nanogenerators (PNGs) was performed in perpendicular to the surface. This imparting pressure on PNGs takes place as a two-step process occurring on its surface. First an object will encounter the surface of the PNG and then it will be compressed it into a compact structure before releasing. When an object (finger imparting) is at a given distance to the surface of the PNGs and it descends, the velocity of that object will increase until it reaches its maximum value before becoming cero as it comes in contact with the surface. A process is illustrated in Figure 13. These two phenomena follow the momentum and kinetic energy theorem, which allows to write the following set of equations:

$$m.g.h = \frac{1}{2}m.v^2(a)$$

$$(F - m.g).\Delta t = m.v(b)$$

$$\sigma = \frac{F}{A}(c)$$

Equations 1 Momentum and kinetic energy equations.

Where *m* is the mass of the average mass of the object, *h* is the falling height and *v* is the maximum velocity the object reaches before reaching the surface of the PNG. *F* is the contact force in a contact area *A* (effective area of the falling object). *Δt* is the average time span between the first contact and the second process in which the PNG will be compacted. This will be the time variation between consecutive voltage peaks.

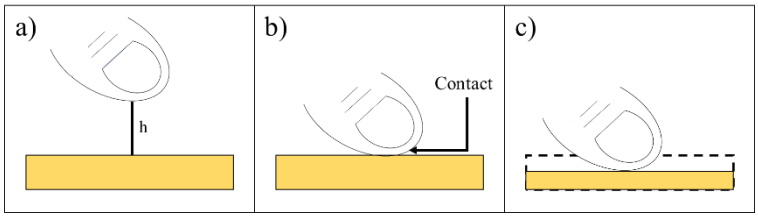

Figure 13 Process by which a double peak was induced by finger imparting force in the surface of the PNG.

3. Results and analysis (1543)

3.1. Structural and physical investigation:

Figure 14 presents the FTIR spectrum of absorption peaks for structures present in the onion skin. From left to right: the wide intense peak at ≈ 3200- 3400 cm-1 is indicative of the —OH stretching of the cellulose present in the samples. Peaks located at 2920 and ≈ 2890 cm-1 coincide with —CH stretching, and the peak observed at ≈ 1750 cm-1 corresponds to carbonyl group (—C=O). The peak at 1596 cm-1 implies the presence of both carboxyl group (—COOH) and —N bending. The presence of carbonyl groups and -N containing bioligands is supported by the peak at 1420 cm-1. At 1236 cm-1 a peak is shown, representing the existence of carbonyl aldehyde (C=O) stretching. Finally, the peaks at 1009 and 850 cm-1 represent C-O stretching and C-O-C asymmetric bending.

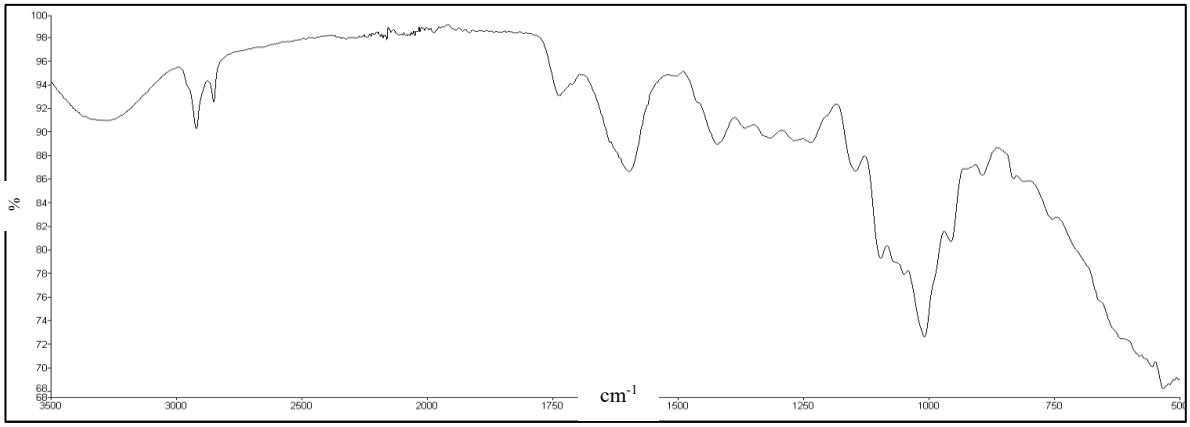

Figure 14 FTIR spectra of onion skin.

Figure 15 presents the FTIR spectrum of absorption peaks for structures present in the CMFs obtained from cotton wads. The peak seen at ≈ 3400- 3125 cm-1 corresponds to the —OH stretching of the cellulose existing in the samples. The peak that goes form 3000-2800 cm-1 indicates the presence of —CH, —CH2 stretching. At 1428 cm-1 —CH —CH2 in-plane bending is observed and the peak at 1325 cm-1 suggests the presence of carbonyl (—C=O) group and -OH vibrations, due to residues of cellulose and hemicellulose. In-plane vibrations of carbonyl group are shown in the peak at ≈ 1175 cm-1, and asymmetric vibrations of the glucose ring is

suggested due to the peak at 1100 cm-1. Lastly the peaks between ≈ 1050- 1000 cm-1 and 880 represent (C-O) stretching and C-O-C asymmetric vibrations, respectively.

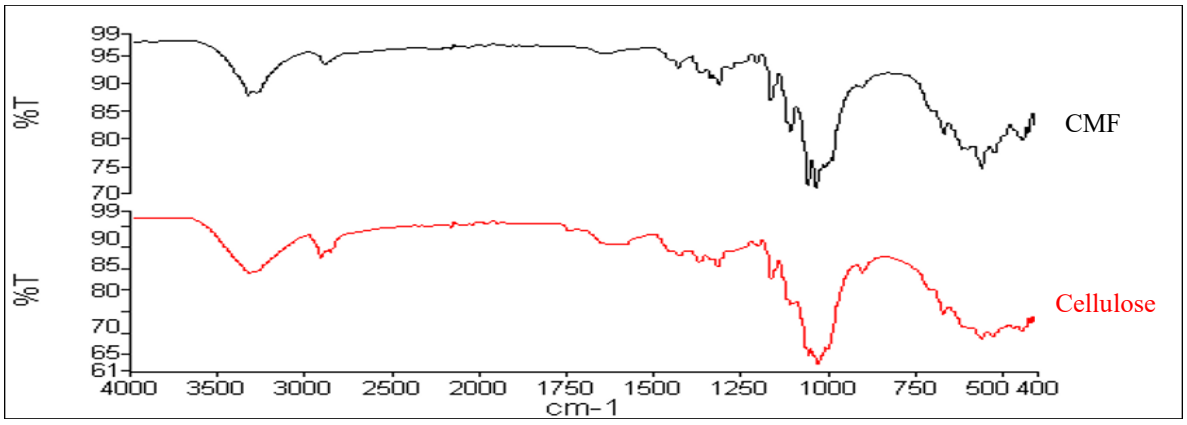

Figure 15 CMF FTIR spectra in comparison with spectra of a laboratory sample of cellulose.

Figure 16 shows the SEM images for onion skin and CMF. The images for the onion skin surface, magnified 520x, shown in Figure 16, indicate the highly aligned tubular shaped cellulose microfibrils in the longitudinal direction. Fiber characterization resulted in an average length of ≈ 518.352 µm, average width of ≈ 42.393 µm and average spacing of ≈ 139.5 µm. Length to width ratio L/D was 12.256. On the other hand, CMF in Figure 16 were magnified 520x and 1000x, respectively. In them, fibrils are disorganized in contrast with those found in OS. The rough surfaces and overall irregular shapes of CMFs are due to the removal of strongly binding materials during the extraction process, contrarily to the smooth surface found in OS images. Fiber characterization resulted in an average length of ≈ 804.222 µm, and average width of ≈ 30.553 µm. Length to

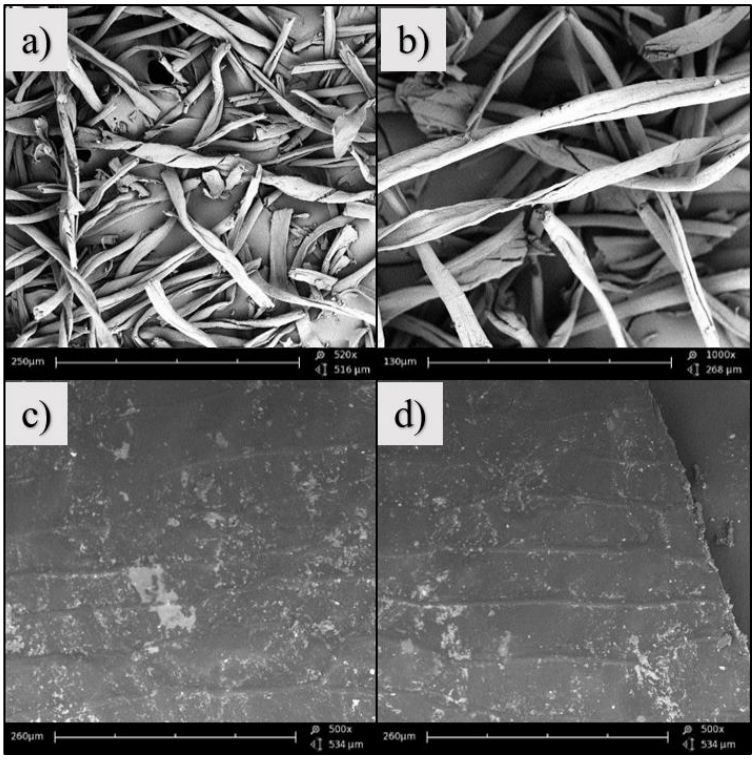

Figure 16 SEM images. a) SEM image of CMF 520x, b) SEM image of CMF 1000x, c) SEM image of OS surface 500x, d) SEM Image of OS surface 500x

width ratio L/D was 26.322. OS fibrils were found to be long and straight overall, whereas the structures of CMFs were found to be curled and twisted, with agglomeration as they are not evenly spaced.

Cellulose presents a complex network structure, as shown in Figure 17, in which various chains are interconnected by the —OH groups of glucose that form strong hydrogen bonds with oxygen atoms in neighboring chains. The hydroxyl groups present in both samples (OS and CMFs) FTIR spectrums Figure 14 Figure 15, respectively, represent the strong hydrogen bonds created along and among the —OH groups of the cellulose fibrils. However as shown in the FTIR results, onion skin is composed of other structures besides cellulose, such as carbonyl and carboxyl groups, -N containing bioligands, and quercetin (brown/reddish colorant in onion skin) [35], [36], on the other hand CMF poses mostly cellulose and other —OH containing structures, mostly hemicellulose and lignin [30]. Al though the nature of piezoelectricity of biomaterials is still not fully understood due to its differences in structure and behavior compared to classic models of piezoelectric theories applied to materials such as ceramics [17], [33]. It is suggested that under mechanical a stress a strong dipole moment created in the surface of the materials due to H-bonding between molecules. Due to the abundance of other molecules and the possibility to have electrostatic interactions between them, it is expected that the behavior of onion skin is entirely different from that of CMF. In addition, the crystalline regions present in the cellulose of the long and self-arranged fibrils observed in the onion skin surface can experience polarization associated with the mechanical stress.

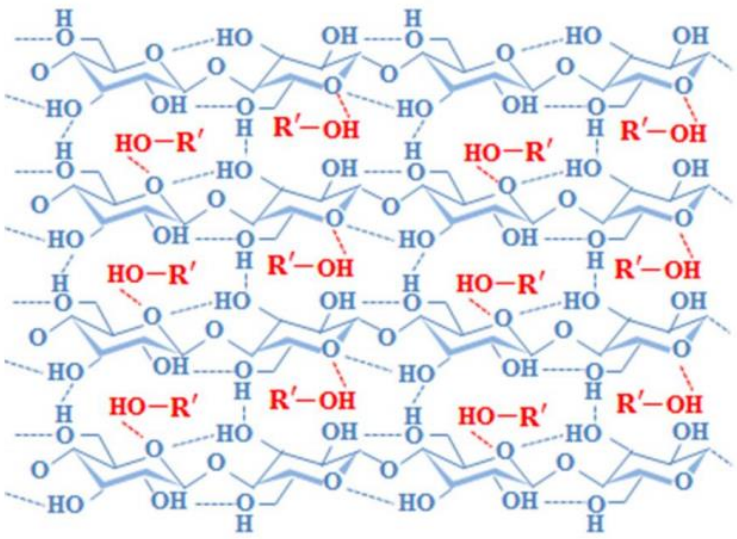

Figure 17 Structure of cellulose after the application of mechanical stress where -OH containing components form interchain H-bonding.

3.2. Piezoelectric nanogenerators

As previously described in sections 2.4 and 2.5, both NOSBPNG and CMFPNG where constructed sharing a common process to add the electrodes and to encapsulate the smart devices. However due to the differences in the material there are still some characteristics that are not shared among them. The area of the PNGs remains the same, 15 mm x 30 mm, however the thickness is different: ≈ 360 nm for NOSBPNG and ≈ 1.99 mm for CMFPNG. Qualitatively, CMFPNG seems more tough than NOSBPNG, and the latter appears to be more flexible. CMFPNG is likely to present more compressive strength due to the drying process of the silicone, which might reduce the chances of having the crystals deformed under pressure, in this sense it is likely a stiffer material than onion skin.

3.3. Electrical characteristics

Experiments were carried to study the behavior of the PNG under different imparting pressures. The output voltage of the PNGs was measured simulating the finger tapping mechanism. Metal cylinders with different weights where dropped form a same height as fingers. Areas and weights are shown in Table 1. The medium cylinder and the tool have two different diameters thus, two areas are reported.

Table 1 Weight, area and description of the metal cylinders.

Image				
Description	Large cylinder	Medium cylinder	Small cylinder	Tool
Weight (kg)	0,78	0,66	0,16	0,10
Area (mm^2)	1.023,54	655,97	314,16	196,07
		1.256,64		254,47

The average falling height (h) for the tool and the small cylinder was ≈ 0,1 m, and for the large and medium cylinders it was ≈ 0,083 m. Using the Equations 1 Momentum and kinetic energy **equations.** it is possible to calculate the force upon impact and the imparted pressure on the device. NOSBPNG generated a voltage of ≈ 1.64 V in open circuit. Results of the output voltage with different pressures are presented in Table 2.

Table 2 Output voltage with different stress

Force, F (N)	Stress, σ (kPa)	Output voltage (V)
10,31	40,53	0,42
10,31	52,60	0,52
16,51	52,56	0,68
62,58	95,40	1,16
62,58	189,63	1,64

The deformation of the material is generated by the extent of axial stress. It is observed that the output voltage depends on the pressure applied to the material. shows the voltage peaks when the material is stress by an external force.

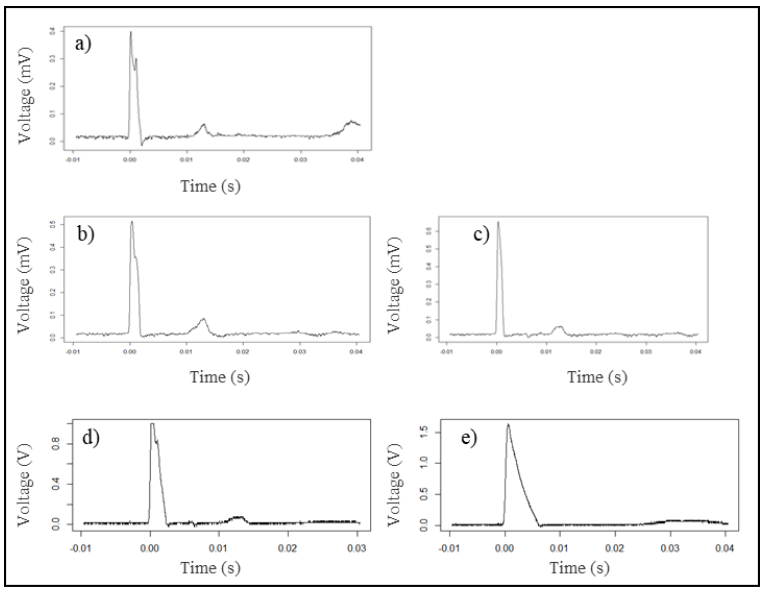

Figure 18 Output voltage NOSBPNG. a) 40.53 kPa, b) 52.60 kPa, c) 52.56 kPa, d) 95.40 kPa, e) 189.63 kPa

The behavior of the NOSBPN under finger imparting was also checked. Figure 19 shows the output voltage. Voltage peaks are not of the same height, due to the uncontrolled impacts of the fingers on the device. However, the height of the peaks, from left to right: 2.04, 0.64, 1.88, 1.52, 2.6, 3.26 V, are similar to those reported in Table 2. Peaks superior to the one 1.64 V obtained on the cylinder tests, suggest that the NOSBPNG can withhold larger pressures. Hence, it is suggested that the imparting pressure is a determining factor in the generation of output voltage through compression and deformation of the crystal structure.

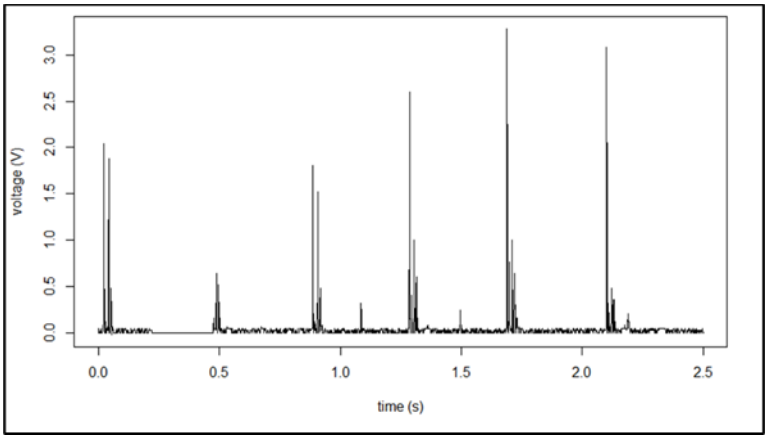

Figure 19 Output voltage generated by finger imparting

3.4. Charging and discharging behavior

To evaluate the potential for power generation in NOSPNG the direct output voltage was stored in a 4.7 µF capacitor, using a circuit as the one shown in Figure 12. Figure 20 shows the charging and discharging behavior of NOSPNGs module[1]. Figure 20 shows a single module under finger imparting that was able to accumulate 22 mV in 50 seconds. To improve the performance of this devices, individual modules were connected in series successfully. Due to the fabrication process, stacking the modules was not possible, instead the individual devices, connected in series, had to be pressed simultaneously. Figure 20b shows two modules in series under finger imparting that were able to accumulate 240 mV in 100 seconds, around one order of magnitude more than with a single module.

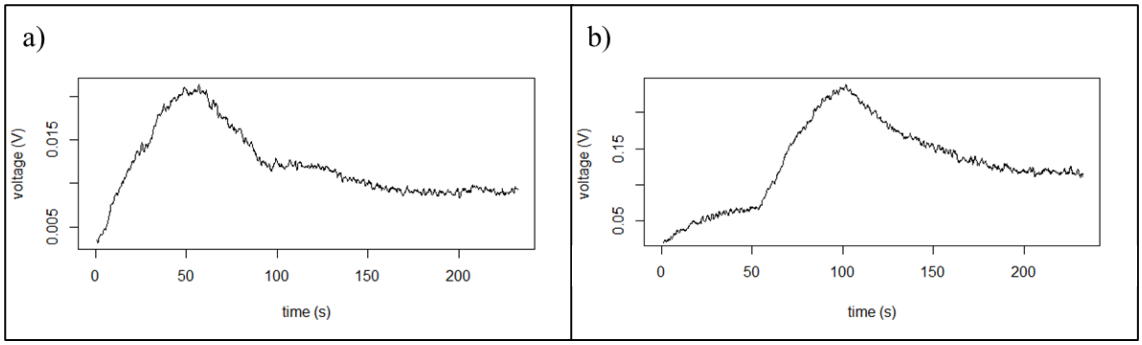

Figure 20 Charging voltage across a 4.7 µF capacitor. a) One NOSBPNG. b) Two NOSBPNG in series.

Due to the fabrication process, stacking the modules was not possible, since between them there was large empty spaces. Instead the individual devices, connected in series, had to be pressed simultaneously and separately. These figures support other experimentation that resulted on the data presented in Table 3. The energy stored was calculated by the equation: $P = \frac{1}{2}.C.V^2$ where C is the capacitance and V is the voltage.

Table 3 Output performance of NOSBPNG

Modules	Time (s)	Voltage (V)	Energy (µJ)
1	120	0,040	0,004
2	120	0,320	0,241
3	120	0,395	0,367
1	50	0,022	0,001
2	100	0,240	0,135

3.5. Device performance discussion

Measuring equipment for this voltage and energy ranges present certain downsides, since the have an internal resistance that consumes the voltage generated by the PNGs. In this line, without the use of a low-noise current amplifier, the measurements of energy and voltage reported could potentially be smaller than those exhibited in real life. In addition to this, real life applications are subject to interferences that can harm the measuring of the performance. Results for CMFPNG where not conclusive and thus not reported.

The methodology used for this investigation is a modification of those reported by [30], [33]. The main modification was the electrode attached to the surface of the materials, both investigations had reported using gold (sputtered) and aluminum, respectively. Sputtered gold electrodes, as the one tested in SOSBPNG exhibit higher charging voltages, 0.5 V on a 10 µF resulted on 1.25 µJ of power stored. However due to constraints in

[1] We call individual NOSBPNG devices modules.

the availability of the material it was decided to use copper tape as the material for the electrode. This material is both thicker and can potentially present separations to the surface, due to irregularities present in the interface. This separation can create an air gap can greatly reduce the potential por power generation in the devices. With respects o CMFPNG, the lack of conducting fillers and the use of a silicone rather than PDMS might have affected the performance of the device, as CMF dispersion in silicone was not homogeneous through mechanical agitation. It is suggested to use mechanisms such as solvent dilution with the addition of conducting fillers to build a homogenous material. It is also relevant to further optimize the ratio of CMF to polymer and the curating time, to allow the maximum flexibility and less stiffness of the material.

4. Conclusions

It was shown that biomaterials exhibit promising characteristics for energy harvesting, as bio-piezoelectric materials. Comparing the chemical and physical structures of these materials indicate the wide number of factors that can be further researched to comprehend the phenomena in bio-piezoelectric materials. Onion skin presents more organized fibers along the longitudinal axis, as well as complex structures, such as quercetin in its conformation that have the potential to form hydrogen bonds between the chains, whereas the simpler, disoriented formation of cellulose microfibrils offers less hydrogen bonding potential and thus a lower power generation. Although the origin of piezoelectricity is not understood for these materials, the present investigation shows an alternative to higher end more expensive materials for the construction of such devices. The implementation of materials such as silicone, contact paper and copper tape, greatly reduce the price and simplify the manufacturing process of such devices. Onion skin, an abundant waste is greatly available as raw material for this kind of smart devices. The self-orientation of its fibers is also of great interest, and its biodegradability makes it a promising material for future research. Present investigation designed a PNG using onion skin without chemical treatment and no sputtering for the formation of the electrode. The NOSBPNG can generate output voltage up until 3.26 V and store 0.395 V in a 4.7 μF capacitor, resulting in a power storage of 1.25 μJ. Furthermore, it was proven that individual modules can be connected in series to increment the power generation in a circuit, allowing for exciting and new possibilities with the current fabrication process of the device. CMFPNG results were not conclusive and suggests that the fabrication process is not adequate for this kind of material, since other aspects of the material must be considered. However, the present investigation also gives notice of important chemical and physical characteristics that can be exploited to pursue the construction of other smart devices.

References

[1] G. M'Boungui, K. Adendorff, R. Naidoo, A. A. Jimoh, and D. E. Okojie, "A hybrid piezoelectric micro-power generator for use in low power applications," *Renew. Sustain. Energy Rev.*, vol. 49, pp. 1136–1144, 2015.

[2] M. T. Todaro *et al.*, "Piezoelectric MEMS vibrational energy harvesters: Advances and outlook," *Microelectron. Eng.*, vol. 183–184, pp. 23–36, 2017.

[3] Z. L. Wang, "Towards self-powered nanosystems: From nanogenerators to nanopiezotronics," *Adv. Funct. Mater.*, vol. 18, no. 22, pp. 3553–3567, 2008.

[4] Y. Han, Y. Feng, Z. Yu, W. Lou, and H. Liu, "A Study on Piezoelectric Energy-Harvesting Wireless Sensor Networks Deployed in a Weak Vibration Environment," *IEEE Sens. J.*, vol. 17, no. 20, pp. 6770–6777, 2017.

[5] M. C. Pacis and R. F. Bersano, "A study on vibration energy harvesting in electric generators," *TENCON 2017 - 2017 IEEE Reg. 10 Conf.*, pp. 3012–3017, 2017.

[6] H. Nesser *et al.*, "All-organic microelectromechanical systems integrating electrostrictive nanocomposite for mechanical energy harvesting," *Nano Energy*, vol. 44, no. August 2017, pp. 1–6, 2018.

[7] S. Priya and D. J. Inman, *Energy harvesting technologies*. 2009.

[8] S. Roundy, M. Strasser, and P. K. Wright, "Powering ambient intelligent networks," *Ambient Intell.*, pp. 271–299, 2005.

[9] S. Kim *et al.*, "Ambient RF energy-harvesting technologies for self-sustainable standalone wireless sensor platforms," *Proc. IEEE*, vol. 102, no. 11, pp. 1649–1666, 2014.

[10] R. Edwards and C. Gould, “Review on micro-energy harvesting technologies,” *Proc. - 2016 51st Int. Univ. Power Eng. Conf. UPEC 2016*, vol. 2017-Janua, pp. 1–5, 2017.
[11] J. Chen and Z. L. Wang, “Reviving Vibration Energy Harvesting and Self-Powered Sensing by a Triboelectric Nanogenerator,” *Joule*, vol. 1, no. 3, pp. 480–521, 2017.
[12] Q. Zheng, B. Shi, Z. Li, and Z. L. Wang, “Recent Progress on Piezoelectric and Triboelectric Energy Harvesters in Biomedical Systems,” *Adv. Sci.*, vol. 4, no. 7, pp. 1–23, 2017.
[13] C. Dagdeviren *et al.*, “Conformal piezoelectric energy harvesting and storage from motions of the heart, lung, and diaphragm,” *Proc. Natl. Acad. Sci.*, vol. 111, no. 5, pp. 1927–1932, 2014.
[14] C. Wei and X. Jing, “A comprehensive review on vibration energy harvesting: Modelling and realization,” *Renew. Sustain. Energy Rev.*, vol. 74, no. February, pp. 1–18, 2017.
[15] A. R. M. Siddique, S. Mahmud, and B. Van Heyst, “A comprehensive review on vibration based micro power generators using electromagnetic and piezoelectric transducer mechanisms,” *Energy Convers. Manag.*, vol. 106, pp. 728–747, 2015.
[16] A. Marino, G. G. Genchi, E. Sinibaldi, and G. Ciofani, “Piezoelectric Effects of Materials on Bio-Interfaces,” *ACS Appl. Mater. Interfaces*, vol. 9, no. 21, pp. 17663–17680, 2017.
[17] S. K. Ghosh *et al.*, “Electrospun gelatin nanofiber based self-powered bio-e-skin for health care monitoring,” *Nano Energy*, vol. 36, no. April, pp. 166–175, 2017.
[18] C. Dagdeviren *et al.*, “Recent progress in flexible and stretchable piezoelectric devices for mechanical energy harvesting, sensing and actuation,” *Extrem. Mech. Lett.*, vol. 9, pp. 269–281, 2016.
[19] S. K. Karan *et al.*, “Nature driven spider silk as high energy conversion efficient bio-piezoelectric nanogenerator,” *Nano Energy*, vol. 49, no. April, pp. 655–666, 2018.
[20] J. Joseph, S. G. Singh, and S. R. K. Vanjari, “Leveraging Innate Piezoelectricity of Ultra-Smooth Silk Thin Films for Flexible and Wearable Sensor Applications,” *IEEE Sens. J.*, vol. 17, no. 24, pp. 8306–8313, 2017.
[21] E. Fukada, “History and Recent Progress in,” *Ultrason. Ferroelectr. Freq. Control. IEEE Trans.*, vol. 47, no. 6, pp. 1277–1290, 2000.
[22] G. Ciofani and A. Menciassi, “Piezoelectric nanomaterials for biomedical applications,” *Vasa*, pp. 467–469, 2012.
[23] C. C. Silva *et al.*, “Collagen-hydroxyapatite films: Piezoelectric properties,” *Mater. Sci. Eng. B Solid-State Mater. Adv. Technol.*, vol. 86, no. 3, pp. 210–218, 2001.
[24] S. Ling *et al.*, “Title: Biopolymer nanofibrils: structure, modeling, preparation, and applications Biopolymer nanofibrils: structure, modeling, preparation, and applications,” *Prog. Polym. Sci.*, 2018.
[25] J. C. Góes, S. D. Figueiró, J. A. C. De Paiva, I. F. De Vasconcelos, and A. S. B. Sombra, “On the piezoelectricity of anionic collagen films,” *J. Phys. Chem. Solids*, vol. 63, no. 3, pp. 465–470, 2002.
[26] E. Praveen, S. Murugan, and K. Jayakumar, “Investigations on the existence of piezoelectric property of a bio-polymer-chitosan and its application in vibration sensors,” *RSC Adv.*, vol. 7, no. 56, pp. 35490–35495, 2017.
[27] K. Kim *et al.*, “Biodegradable, electro-active chitin nanofiber films for flexible piezoelectric transducers,” *Nano Energy*, vol. 48, no. March, pp. 275–283, 2018.
[28] Q. Zheng, H. Zhang, H. Mi, Z. Cai, Z. Ma, and S. Gong, “High-performance flexible piezoelectric nanogenerators consisting of porous cellulose nanofibril (CNF)/poly(dimethylsiloxane) (PDMS) aerogel films,” *Nano Energy*, vol. 26, pp. 504–512, 2016.
[29] L. Csoka, I. C. Hoeger, O. J. Rojas, I. Peszlen, J. J. Pawlak, and P. N. Peralta, “Piezoelectric effect of cellulose nanocrystals thin films,” *ACS Macro Lett.*, vol. 1, no. 7, pp. 867–870, 2012.
[30] M. M. Alam and D. Mandal, “Native Cellulose Microfiber-Based Hybrid Piezoelectric Generator for Mechanical Energy Harvesting Utility,” *ACS Appl. Mater. Interfaces*, vol. 8, no. 3, pp. 1555–1558, 2016.
[31] S. Rajala *et al.*, “Cellulose Nanofibril Film as a Piezoelectric Sensor Material,” *ACS Appl. Mater. Interfaces*, vol. 8, no. 24, pp. 15607–15614, 2016.
[32] K. Rahbar Shamskar, H. Heidari, and A. Rashidi, “Preparation and evaluation of nanocrystalline cellulose aerogels from raw cotton and cotton stalk,” *Ind. Crops Prod.*, vol. 93, pp. 203–211, 2016.
[33] S. Maiti, S. Kumar Karan, J. Lee, A. Kumar Mishra, B. Bhusan Khatua, and J. Kon Kim, “Bio-waste onion skin as an innovative nature-driven piezoelectric material with high energy conversion efficiency,” *Nano Energy*, vol. 42, no. July, pp. 282–293, 2017.

[34] M. P. Wolf, G. B. Salieb-beugelaar, and P. Hunziker, “Progress in Polymer Science PDMS with designer functionalities — Properties , modifications strategies , and applications,” *Prog. Polym. Sci.*, vol. 83, pp. 97–134, 2018.
[35] O. T. Ifesan, Beatrice, “Chemical Composition of Onion Peel (Allium cepa) and its Ability to Serve as a Preservative in Cooked Beef,” *IJSRM.Human*, vol. 7, no. 4, pp. 25–34, 2017.
[36] V. Benítez *et al.*, “Characterization of Industrial Onion Wastes (Allium cepa L .): Dietary Fibre and Bioactive Compounds,” pp. 48–57, 2011.